Materials Science Forum
ISSN: 1662-9752, Vol. 1087, pp 115-126
doi:10.4028/p-wxko9z
© 2023 Trans Tech Publications Ltd, Switzerland
Submitted: 2022-10-31
Revised: 2023-01-26
Accepted: 2023-02-06
Online: 2023-05-12

Bonding Characteristics of Grey Cast Iron and Microalloyed Steel Using Furnace Brazing

Marios Kyprianidis[1,a], Dimitra Ioannidou[1,b], Angelos Kaldellis[1,c], Vassilis Stergiou[2,d], Petros E. Tsakiridis[1,e*]

[1]School of Mining and Metallurgical Engineering, National Technical University of Athens, Greece.

[2]Special Processes and Materials Technology Department, Hellenic Aerospace Industry, Schimatari, Greece

[a]marios.kyprianidis@outlook.com, [b]dimitraioannidou.96@gmail.com, [c]aggkald@gmail.com, [d]stergiouvas@yahoo.gr, [e]ptsakiri@central.ntua.gr

Keywords: Brazing, Cast Iron, Microalloyed Steel, Microstructure, Corrosion.

Abstract. The present research work focuses on the study of the microstructure evolution, corrosion resistance, and mechanical properties of GG25 grey cast iron and AISI 4140 micro-alloyed steel dissimilar brazing joints, using a eutectic type Ag-based filler metal. The welding zone microstructure study was carried out through optical (OM) and scanning electron microscopy (SEM), in conjunction with an energy-dispersive X-ray detector (EDS). Joints' mechanical properties were investigated through tensile tests, as well as detecting the Vickers microhardness across the microstructure's zones. For the assessment of the joints' corrosion resistance, potentiodynamic polarization tests were performed in 3.5 wt% NaCl solution, at various temperatures. The corrosion products evaluation was carried out by both X-ray Diffraction (XRD) and scanning electron microscopy (SEM). According to the results, a sound brazing joint was attained, presenting an average tensile strength and ductility of about 230 MPa and 20 %, respectively.

1. Introduction

Gray cast irons, containing more than 2 wt% carbon, 1 to 3 wt% silicon, and up to 1 wt% manganese, are the most versatile and widely used cast irons. They are materials of increasing importance in the manufacturing industry because of their high castability, hardness and wear resistance, corrosion resistance, machinability, low melting point, and also being cost-effective. Moreover, these alloys are an important engineering and structural group of materials and they have been widely used in machine components manufacturing, such as engine blocks, disc brake rotors, hydraulic valves, etc. [1, 2].

Gray cast iron's structure consists of branched and interconnected graphite flakes in a matrix that is pearlitic, ferritic, or a mixture of them. When molten pig iron is cooling slowly down, much of the carbon is separated in the form of tiny graphite flakes, scattered throughout the matrix, forming planes of weakness, which basically control the mechanical properties and result in relatively low strength and toughness. Their presence causes also the gray appearance of the fracture, which characterizes ordinary gray cast iron. Commercial gray cast irons contain 2.0 to 4.5 wt% carbon and in order to obtain a graphitic microstructure, silicon should be present (1-3%wt), since in contrast to white cast iron, Si is a graphite stabilizing agent and leads to the graphite formation avoiding the corresponding of iron carbides. In a higher percentage of silicon (≈3 wt%) almost no carbon is held in the form of carbides [3, 4]. The alloy graphitization is also depending on the solidification rate. In case of slower cooling rates, the carbon is diffused and accumulated in the form of graphite flakes. A moderate cooling rate forms a pearlitic matrix, whereas rapid cooling suppresses graphitization and leads to the development of a ferritic matrix in conjunction with cementite (white iron). The manganese content varies as a function of the desired matrix (as low as 0.1 wt% Mn in ferritic gray irons and as high as 1.2 wt% in pearlitic). Increasing the manganese content tends to promote the formation of pearlite while cooling through the critical range. Nevertheless, it should be noted that only the percentage of Mn, which is not combined with S, is effective. The usual microstructure of gray cast iron is a matrix

All rights reserved. No part of contents of this paper may be reproduced or transmitted in any form or by any means without the written permission of Trans Tech Publications Ltd, www.scientific.net. (#628746377, CERN Library, Geneva, Switzerland-04/12/23,11:11:20)

of pearlite with graphite flakes dispersed throughout. Foundry practice can be varied so that nucleation and growth of graphite flakes occur in a pattern that enhances the desired properties [4, 5].

Cast irons are generally considered difficult materials to be welded. Their weldability mainly depends on microstructure and mechanical properties. Gray cast iron, whose lack of ductility is caused by the coarse graphite flakes, is an inherently brittle material and often cannot withstand stresses, set up by cooling during welding. On the other hand, the graphite clusters in malleable irons, and the nodular graphite in spheroidal graphite or ductile cast irons, give significantly higher ductility which improves weldability. Gray cast iron weldability is mainly aggravated due to the development of hard and brittle microstructures in the heat-affected zone (HAZ) and partially in the fusion zone (FZ). During the fast solidification, the major proportion of the carbon precipitates in the form of cementite, while the austenite to pearlite/ferrite transformation has not proceeded and the microstructure of the HAZ has consisted of martensite with some retained austenite [6-8].

Brazing is a joining technique for metals or ceramics, using a metal with a lower melting point than either of the materials to be joined. The melted filler metal flows in between the joined parts to produce a strong and leakproof connection. The effect of this process is known as capillary action and it enables penetration between the metallic surfaces to be joined. The capillary effect is based on the principle of surface tension and it is the ability of a liquid (the molten filler metal) to flow in narrow gaps without the help of external forces, even against gravity. In the brazing process, it is assured that the filler rises, because of this capillary force, into the gaps between the parts to be joined and up to the top side of the assembly to wet the area, and to finally form the joints and the fillets expected. The imperfections and the irregularities between the metals to be joined create channels, along which the molten filler metal can move and the phenomenon of the force that pulls it through the microscopic pores is called capillary action. To meet this requirement, the filler metal must have a melting point above 450 ^{o}C, but below the melting point of the base metals [9-11].

Furnace brazing is an industrial, high-volume, semi-automated process, which allows manufacturing engineers to join simple or complex designs of one-joint or multi-joint assemblies. The process offers the benefits of a controlled heat cycle (allowing the use of parts that might distort under localized heating) and no need for post-braze cleaning. During the process, the whole assembly is heated to a temperature where the braze alloy melts and flows into the joint. On subsequent cooling it freezes, making a solid joint. In furnace brazing operations many thousands of joints can be made at the same time. The main advantages of furnace brazing include the possibility to braze dissimilar materials, greater control over tolerances, and avoidance of distortion in the finished piece. The main disadvantages of braze welding are the reduced strength and heat resistance of the filler metal [12-14].

Brazing is preferred in the case of cast iron joints since inputs less heat in the casting and lowers by far the chances of cracking compared to traditional welding techniques. Because braze welding needs a lower temperature to melt only the filler metal and doesn't melt the base cast iron, rapid expansion and, as a result, immediate cracking due to the expansion forces, is prevented. Furthermore, it prevents the generation of residual stresses remaining in the base metal and the consequent changing of the casting's characteristics. On the other hand, because most cast iron reforms are small repairs, braze welding is more suitable and offers more advantages than fusion welding, especially because of the reduced cracking risk and the corresponding heat-affected zone metallurgical alterations [15-17].

The so far published literature has given little attention to the dissimilar bonding characteristics between grey cast irons and micro-alloyed steels, through furnace brazing. The current investigation focuses on the comparison between microstructure and metallurgical changes in the HAZ, corrosion resistance, and mechanical properties of GG25 grey cast iron and AISI 4140 low alloy steel dissimilar furnace brazing joints, using a eutectic type Ag-base filler metal.

2. Experimental

2.1. Materials and Procedure for Brazing Tests. Dissimilar joints of GG25 gray cast iron (Traid Villarroya, Spain) to AISI 4140 (German Grade: 42CrMo4) low alloy steel (Dorrenberg Edelstahl GmbH, Germany), was carried out by furnace brazing using a suitable low-melting Ag alloy braze filler with high fluidity and filling properties. The nominal composition of both materials is given in Table 1.

Table 1. The nominal composition of base metals [wt%]

Base Metal	*C*	*Si*	*Mn*	*Cr*	*Mo*	*S*	*P*	*Cu*	*Ni*	*Fe*
GG25	3.17	2.01	0.70	0.07	0.005	0.245	0.018	0.545	0.014	Balance
AISI 410	0.40	0.33	0.93	1.12	0.18	0.031	0.025	0.02	0.17	Balance

The Ag-Cu-Zn-Cd brazing filler metal (Easy Flo, Lucas Milhaupt, USA) used in the present investigation with 50 wt% of silver (Table 2), has been widely used, as is less sensitive to the rate of heating, mainly due to its narrow melting range. Its solidus and liquidus temperatures are 626 ºC and 635 ºC, respectively.

Table 2. The nominal composition of brazing filler alloy [wt%]

Filler Type	*Ag*	*Cu*	*Zn*	*Cd*
Ag-Cu-Zn-Cd	50.07	15.55	16.58	17.17

It is a eutectic type, free-flowing filler metal, which is not separated into low and high melting constituents, with high fluidity, which makes well-fitted joints essential and prevents ‘bridging’ or large fillet formation. It is a general-purpose braze filler metal, forms strong joints with stable strength up to 425 ºC and can be used successfully for joining most ferrous and non-ferrous alloys. Due to its high silver content, it has more resistance to corrosion in chlorine, sulfur and steam environments. However, the corrosion behavior of the whole joined component is challenging and it is critical to investigate it.

The filler was used in the form of Ø 1 mm wire. Pre-formed filler brazing is generally the most suitable solution in situations when distribution and repeatability are of paramount consideration. The recommended brazing temperature ranges between 635 ºC - 746 ºC.

Flow, wetting and spreading of liquid filler are affected by the presence of oxides and impurities present at the surfaces to be brazed. For removing the oxides proper cleaning methods are used including mechanical cleaning. Additionally, in the case of gray cast iron brazing, it is necessary to treat the surface prior to brazing to remove the graphite. This will ensure good wetting by the brazing filler metal. For this reason, the cast iron surface to be brazed was heated to 500 °C using an oxyacetylene torch flame for 15 minutes.

The key to successful brazing is joint design. Because the process depends on capillary attraction, the spacing between the parts to be joined must be small and accurately controlled. In the present investigation a socket (tube) joint of brazing of a bushing, made from an AISI 4140 low alloy steel, into a GG25 gray cast iron sleeve, was examined.

A tube joint should be designed to be strong enough to carry loads such as pressure, dead weight, and thermal expansion. Figure 1 shows the above socket-type fitting joint, between the steel tube and the gray cast iron, which is a kind of lap joint. The two parts intended for brazing were laid on top of each, and the capillary spacing between the two pieces comprised the braze joint when the filler metal melts and flows. The joint strength of a brazed lap joint is a function of overlap distance and the thickness of the brazed joint itself. The gap between the two parts is usually in the range of 50-150 μm.

Prior to brazing preparation, all surfaces were cleaned using acetone. After placement of filler metal, a special flux, the mixture of boric acid and fluoride compounds, was applied on the filler

metal, in order to obtain better wetting and bonding. The main purpose of the flux is to remove any oxides from the surfaces of the parts or prevent oxidation during heating to brazing temperature.

Furnace brazing was performed at atmospheric conditions. Generally, heating should be carried out at a temperature of 50 °C above the melting point of the filler alloy, with a duration of a few minutes. In this case, the parts were heated up to 710 ºC (heating rate: 11.5 ºC/min). Parts were maintained at this temperature for approximately 5 minutes and then cooled to room temperature.

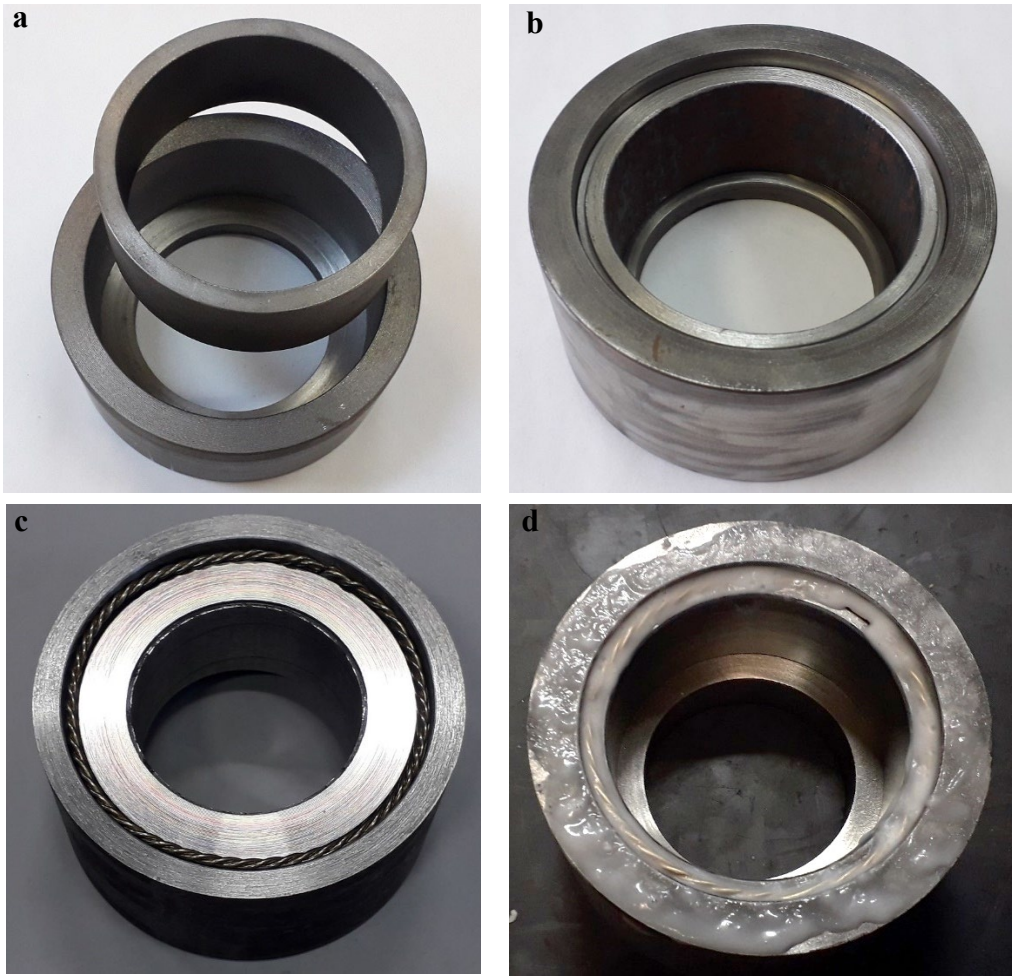

Fig. 1. GG25 grey cast iron and AISI 4140 low alloy steel dissimilar socket brazing joint

2.2. Brazing Joints Characterization. Representative samples of the brazed joint were cut using a precise microtome (Struers Accutom-2, Denmark), followed by a standard metallographic procedure. Microstructure characterization was performed on the cross-section of the brazed joints, in polished sections after etching with Nital reagent. The samples after being impregnated in a low-viscosity epoxy resin (Akasel Denmark) under vacuum were cut via micro-saw and then ground and polished down to 1 μm diamond paste on a lapping disk.

The microstructural observation was initially carried out in an Olympus BX41M optical microscope (Japan) and then, with a Jeol 6380 LV scanning electron microscope (Japan), using both secondary and backscattered electron detectors. Microanalyses, in order to identify the phases constitution of the braze alloy and brazed joint, was accomplished with an Oxford INCA (UK) energy dispersive spectrometer (EDS) connected to the SEM.

To assess the mechanical properties of the dissimilar joint under investigation, stress-strain curves from uniaxial quasi-static tensile tests were constructed in accordance with ASTM E8M [18], using a universal testing machine (Instron 84482, UK) with 100 kN load cell, at a loading rate of 1 mm/min. The entire cross-section was used to estimate the nominal stress.

Microhardness testing was conducted in accordance with ASTM E384 [19], using an HV-1000 (China) microhardness tester implementing 100 gf for 15 seconds. The braze zone, heat-affected zone

(HAZ) and base metal (BM) were covered during the microhardness test and then correlated with the microstructural observations.

To evaluate the corrosion behavior of the braze joints, potentiodynamic polarization tests were carried out in an electrolyte of 3.5 wt% NaCl, at 25, 50 and 80 ºC (±2 ºC). The solution was prepared by using distilled water and analytical grade NaCl. The selected samples, extracted from the brazed zone, as the working electrode, a saturated calomel electrode (SCE) as the reference electrode, and graphite as the counter electrodes were combined in a conventional three-electrode cell. The experiments were conducted in accordance with ASTM G5 [20], using an Amel Potentiostat/Galvanostat Model 2551 (Italy), with VApeak software. An open circuit potential was established within 15 min, before the electrochemical tests. After that, a polarization test was performed at a scanning rate of 0.1 mV/s from -250 to +1600 mV. The produced potentiodynamic curves were used to designate the corrosion potential, corrosion current density and the slope of the anodic and cathode curve of the tested materials.

The phase identification of the corrosion products was carried out using a Bruker D8-Focus (Germany) diffractometer with nickel-filtered CuKa radiation (λ=1.5406 Å), at 40 kV and 40 mA. SEM analysis was also used in order to detect the morphology and the composition of the developed corrosion products, on the surface of the corroded samples.

3. Results and Discussion

The microstructural characteristics of the braze joint zone, along with the heat-affected zone and the corresponding base metals were examined under an optical and scanning electron microscope in polished and etched sections (Fig. 2 and 3).

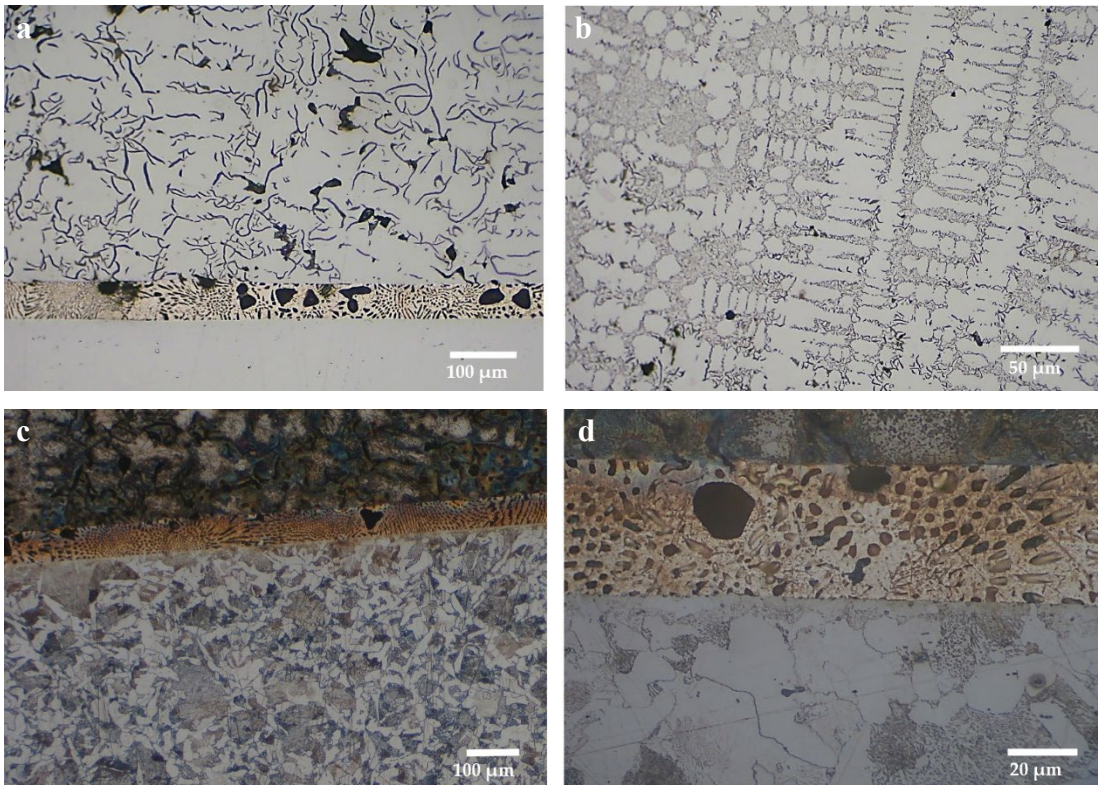

Fig. 2. Representative micrographs, under OM, of AISI 4140 low alloy steel (down) – GG25 gray cast iron (up) joints brazed with Ag-Cu-Zn-Cd brazing filler alloy

Although gray cast iron is the least brazeable of the cast irons, as it forms large graphite flakes that inhibit the wetting of the metal surface, the filler metal in all cases exhibited good wettability on both base metals. The joint interfaces were sound, no defects appeared at the brazing seam and no pores were detected near the interface with the parent materials. Its spreading behavior did not produce any cracking tendency.

The phases present in the molten metal have a mainly spherical shape, but also needle-like shape forms were observed, due to the cooling conditions. The size of the heat-affected zone was quite limited, about 300 μm for cast iron and 50 μm for steel, mainly due to the mediate brazing temperature. According to the SEM micrographs provided and the corresponding EDS analyses, the microstructure of the brazed joint constituted two discernible phases (Fig. 3).

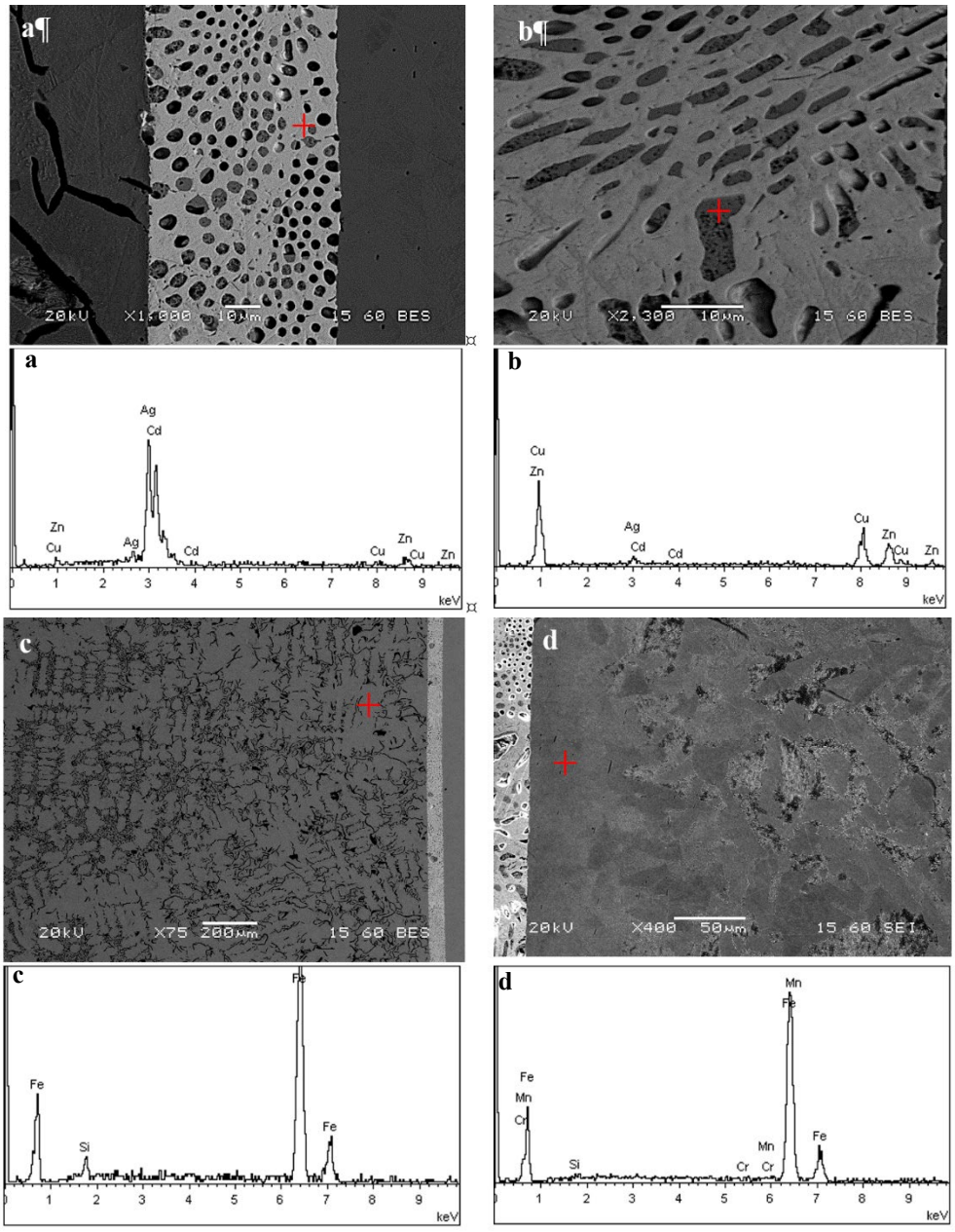

Fig. 3. Backscattered electron micrographs and microanalyses; a: joints brazed with Ag-Cu-Zn-Cd b: joints brazed with Ag-Cu-Zn-Cd, c: GG25 gray cast iron d: AISI 4140 low alloy steel

The matrix of the joint, an Ag solid solution, rich in Cd, and a Cu phase (solid solution) rich in Zn, which was uniformly distributed inside the silver matrix. Cu and Zn (with similar atomic radius) are in the same element period, whereas Ag and Zn are in a different one. Similarly, Ag and Cd (with also similar atomic radius) are in the same element period. As a result, the solubility of Zn in Cu is much higher than the corresponding Zn in Ag, and correspondingly the solubility of Cd in Ag is much higher than the corresponding Cd in Cu. Therefore, as the temperature was decreased, the solid solution composed of Cu and Zn, presenting a higher melting point, crystallized first, inside the liquid matrix of silver and cadmium solid solution.

The microstructure of GG25 gray cast iron consists of a high density of graphite flakes, due to high silicon content, formed during the solidification process, which is uniformly distributed in a pearlitic structure matrix. During the brazing process, the temperature reached at 710 ºC, followed by air cooling. The graphite flakes in the HAZ seemed to be coarsened, whereas the corresponding average lamellar spacing of pearlite was increased. This observation should be attributed to the temperature increment in the HAZ near the joint seam. The graphitization process depends on both alloy heat treatment and the consequent cooling rate, as the carbon is diffused from the perlite grains and is accumulated in pre-existed finer graphite flakes [3, 4]. As the distance between the lamellas in the pearlite increased the mechanical properties of the material decreased.

Regarding the microstructure of the heat affected zone (HAZ) at the interface of 4140 steel base metal and the brazed joint, consists of relatively coarse ferrite with dispersed carbides, in the form of both rod and spheroidal shape. During heating the carbides precipitate in the martensite, transforming the microstructure to tempered martensite. However, the grains near to the weld zone were undergoing higher peak temperatures, probably in the range of 600-650 ºC and consequently, they were recrystallized. This observation was also confirmed and by the existence of spheroidal shape carbides, mainly cementite, which are developed during the martensite transformation, to ferrite and carbides, in the temperature area of 550 and 650 ºC [21].

The microhardness profiling of the brazed joint, along with the corresponding base metals, carried out at a depth zone of 3 mm on either side, is presented in Figure 4. The average Vickers microhardness values of the parent materials, GG25 gray cast iron and AISI 4140 low alloy steel were HV 265 and HV 230, respectively. As expected, the hardness values of the brazing joint were significantly lower than that of the base metals. The mean microhardness of the lowest point was 190 HV.

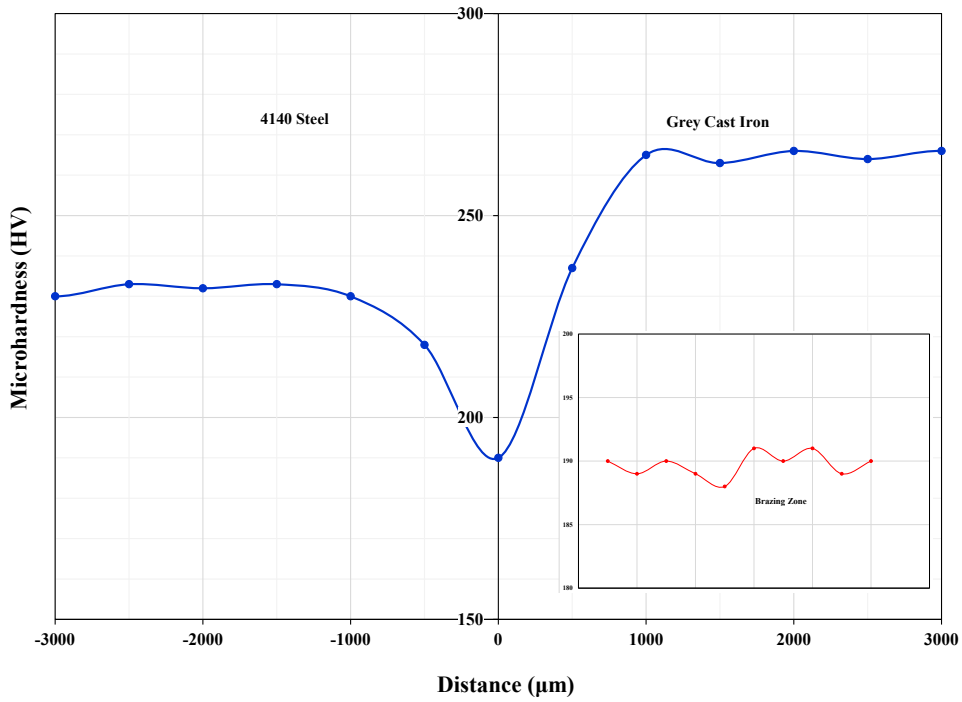

Fig. 4. Base metals and brazing joint microhardness

The microhardness values in the heat affected zone was relatively lower for both cast iron and steel, indicating that a softening takes place in that particular zone, during brazing. After melting and solidification of the brazed alloy, the strengthening effect of the base metals due to recrystallization phenomena is lost. As it was mentioned above, the pearlitic zone in the case of cast iron, presented a morphology with wider lamellas, aggravating the mechanical properties of the interface. Similarly, in the case of low alloy steel, its heat-affected zone consists of relatively coarse ferrite grains with rod and spheroidal shape carbides, which led to the decrement of the microhardness values.

The corresponding engineering stress-strain curves obtained from the tensile tests are presented in Figure 5. The average tensile values at failure were calculated by dividing the breaking load by the product of the base metal thickness and the sample width. The results demonstrated satisfactory tensile strength. Typical elastic-plastic deformation was observed. The average tensile strength of the brazing joint was determined at about 230 MPa, presenting an average ductility (in terms of percent elongation) in the range of 18-22 %. The applied furnace brazing process led to joint interfaces with no defects with good wettability on both base metals.

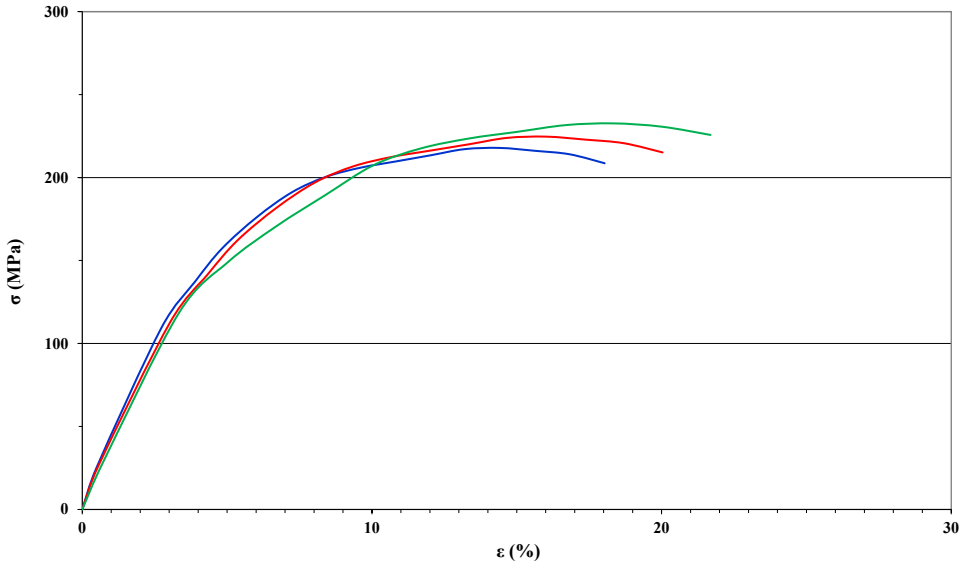

Fig. 5. Stress-strain curves of grey cast iron/low alloy steel dissimilar brazing joints

Potentiodynamic polarization tests were carried out in an electrolyte of 3.5 wt% NaCl, at 25, 50 and 80 °C (±2 °C) in both base metals and braze joints. The corresponding curves after exposure in the area of the brazing seam are presented in Figure 6. Both anodic and cathodic reactions were enhanced due to the increased temperature. It was revealed that with the decrement of the electrolyte temperature, the corrosion current density (I_{corr}) decreased and the corrosion potential (E_{corr}) shifted to a more cathodic side. The sample exposed to 80 °C presented the lowest Ecorr and the highest current density. It is known that the higher the E_{corr} and the lower the I_{corr}, the better the corrosion resistance is. A higher electrolyte temperature led to a higher corrosion rate since the corrosion reactions are temperature-dependent for the most active alloys.

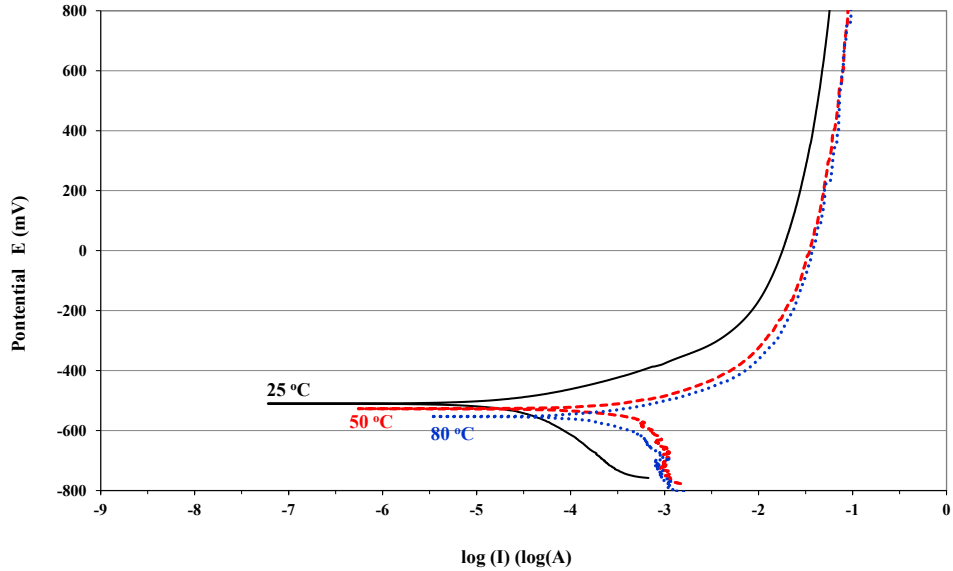

Fig. 6. Brazed joints potentiodynamic polarization curves in 3.5 wt.% NaCl at various temperatures

The increase of temperature increased the surface activation and promoted the brazed matrix dissolution. As the immersion temperature increased, the I_{corr} in all cases gradually increased, indicating that the corrosion rate also increased, since the temperature is the driving force for ion diffusion, and the corrosion rate accelerated as the temperature raised.

The corrosion product's phase identification, developed during potentiodynamic polarization on the brazing seam surface, at various temperatures, was investigated via X-ray diffraction (Fig. 7).

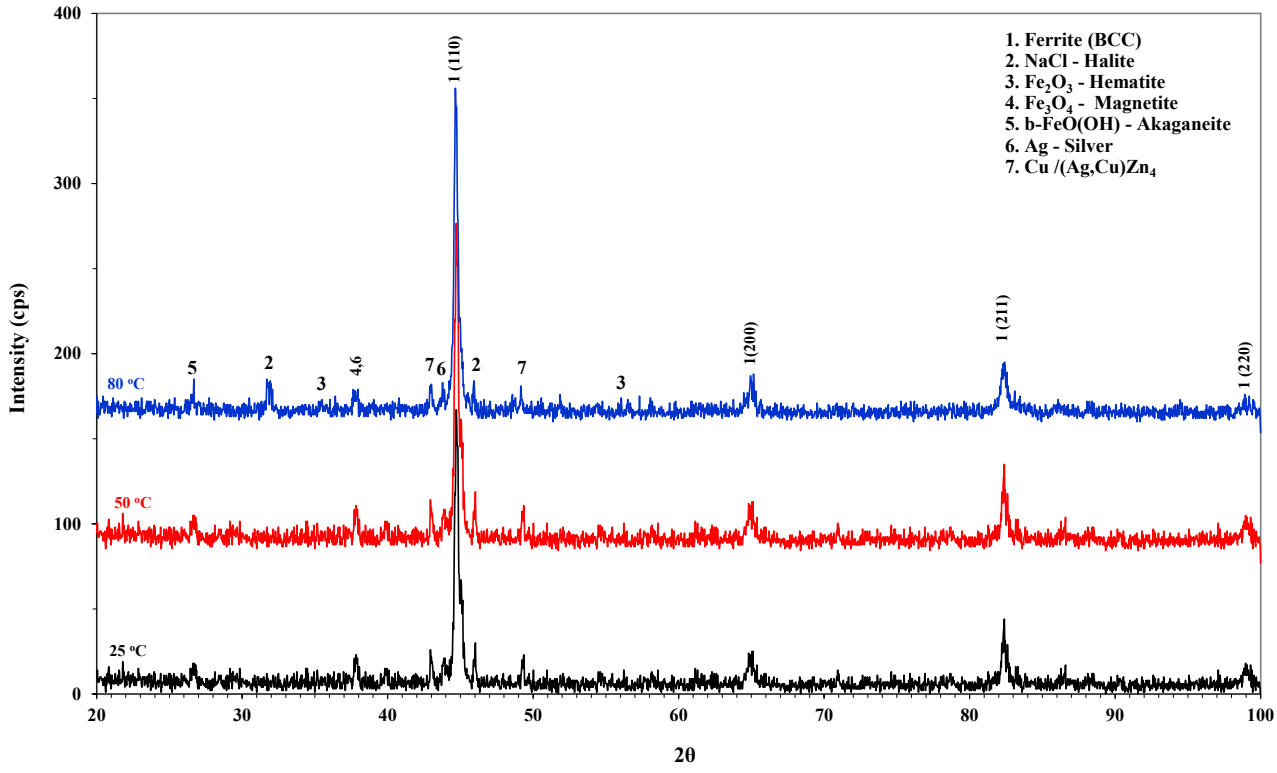

Fig. 7. XRD patterns of corroded brazing joints in 3.5 wt.% NaCl at various temperatures

According to the results, the composition of corrosion products did not alter significantly due to temperature variations. The detection of the typical iron corrosion products, hematite (Fe_2O_3), magnetite (Fe_3O_4) and akagaenite (β-FeOOH), have been produced and partially covered the brazed joint during the corrosion of both gray cast iron and low alloy steel base metals. The detection of iron substrates showed reflections corresponding to a 44.76° (110), 65.05° (200), 82.29° (211), and 98.66° (220), with the (110) orientation exhibiting the greatest diffraction intensity.

The above results were also confirmed during the corrosion products examination under the scanning electron microscope, in conjunction with an energy dispersive spectrometer (EDS) (Fig. 8). The distribution of the corrosion product on the brazed joints surface was also investigated by SEM. In all cases, the morphology of pitting cavities has been observed in the area of the Cu-Zn solid solution phase, which was increased with the temperature increment.

On the other hand, the Ag matrix seems to suffer less, since no silver corrosion products were detected. Silver becomes passive in most halide solutions, because of the formation of a very thin halide layer. The copper solid solution on the brazed joint, with about 45 wt% of zinc, has suffered from dealloying via a mechanism called dezincification, when Zn is selectively dissolved out of the Cu-Zn matrix, leaving behind a porous Cu-enriched surface layer. This phenomenon can lead to brittle crack nucleation sites and mechanical failures, as well as the release of other alloying elements.

This observation was confirmed and by the detection of $ZnCl_2$ salt, on the surface of the brazed joints and especially on the Cu-Zn phase. Zn has a high tendency to dissolve, whereas copper has a high tendency to be reduced. The E° for zinc is –763 mV, whereas the E° for copper is 337 mV, which shows the above tendencies.

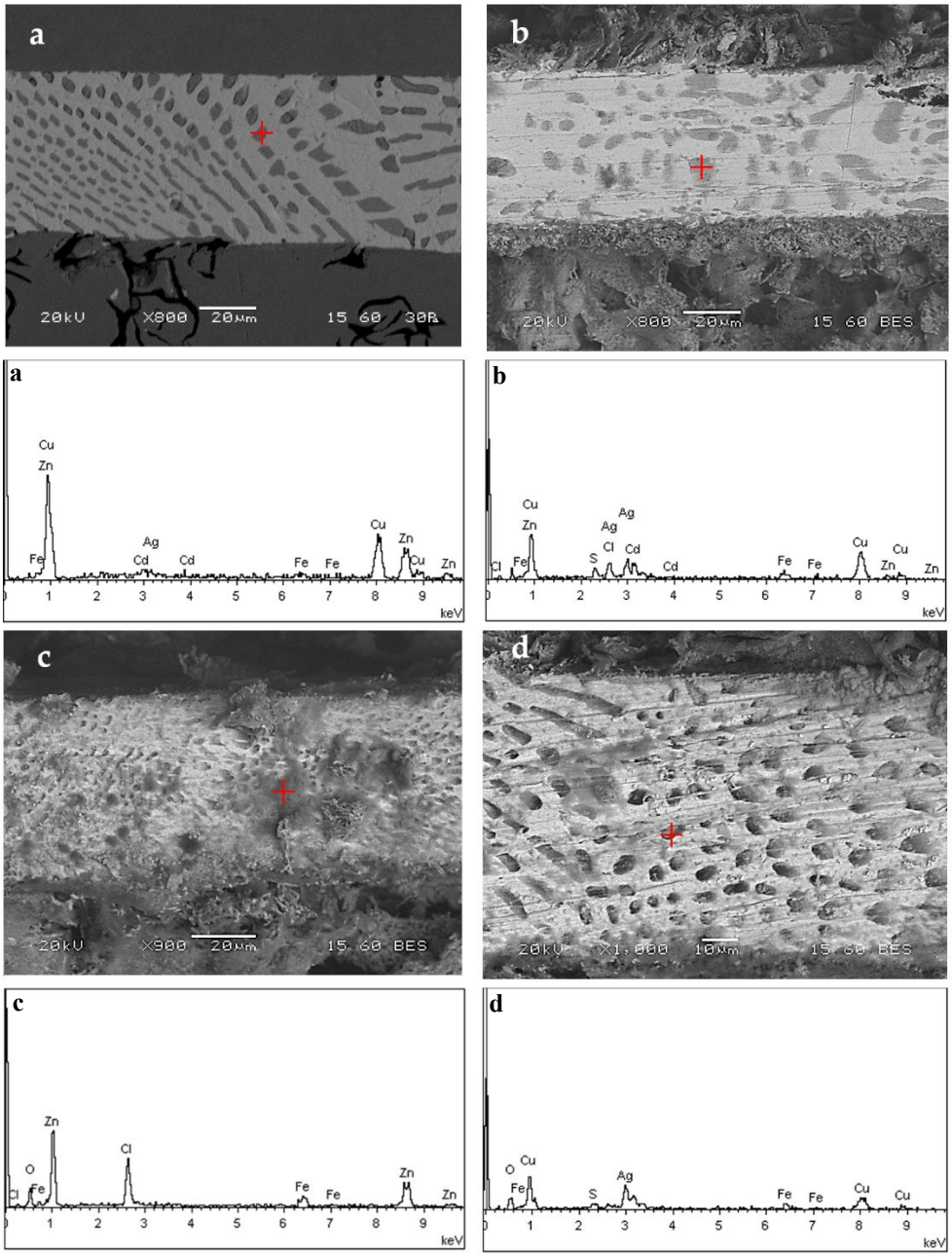

Fig. 8. Micrographs and EDS analysis. (a) As Received, (b) 25 °C, (c) 50 °C, and (d) 80 °C

The less noble atoms dissolution (Zn) was initiated within a distance of several atoms from the reaction front (surface). Short-range dissolution allowed a gradual formation of interconnected paths of the less noble element in a CuZn binary phase, thus permitting the continuity of selective leaching from the surface to a certain depth. The alloy has been mechanically weakened to the extent that a slight increase in the load could lead to a failure initiation.

Conclusions

In the present research study, the microstructure evolution, mechanical properties, and corrosion resistance of GG25/AISI 4140 dissimilar furnace brazing joints, using a eutectic type Ag-base filler alloy were systemically studied and the following conclusions have been made:

- In all cases proper wettability between the filler alloy and both base metals was observed. The microstructure of brazed joints constituted two phases. The matrix of the joints consisted of an Ag solid solution rich in Cd, and a Cu phase (solid solution) rich in Zn, which was uniformly distributed inside the silver matrix.

- The size of the heat-affected zone was quite limited, about 300 μm for cast iron and 50 μm for steel, mainly due to the mediate brazing temperature. The graphite flakes in the HAZ were coarsened, whereas the corresponding average lamellar spacing of pearlite was increased. On the other hand, the heat-affected zone (HAZ) of steel consisted of relatively coarse ferrite with dispersed carbides, in the form of both rod and spheroidal shape mainly due to the martensite transformation in the temperature range of 600-650 °C.
- The average tensile strength of the brazing joint was determined at about 230 MPa, presenting an average ductility of about 20 %.
- Potentiodynamic polarization tests of the brazed joints at various temperatures, both anodic and cathodic reactions were enhanced in relation to the temperature increment.

References

[1] J.A.G. de Sousa, W.F. Sales, A.R. Machado, A review on the machining of cast irons, J. Adv. Manuf. Technol. 94 (2018) 4073-4092.

[2] H. Zhang, D. Liu, L. Zhao, J. Wang, S. Xie, S. Liu, P. Lin, X. Zhang, C. Chen, Review on corrosion and corrosion scale formation upon unlined cast iron pipes in drinking water distribution systems, J. Environ. Sci. 117 (2022) 173-189.

[3] L. Collini, G. Nicoletto, R. Konecna, Microstructure and mechanical properties of pearlitic gray cast iron, Mater. Sci. Eng. A. 488 (2008) 529-539.

[4] J.R. Davis, ASM Specialty Handbook: Cast Irons, ASM International, 1996

[5] A. Sadeghi, A. Moloodi, M. Golestanipour, M.M. Shahri, An investigation of abrasive wear and corrosion behavior of surface repair of gray cast iron by SMAW, J. Mater. Res. Technol. 6 (2017) 90-95.

[6] G.B. Dutra, U. Tetzlaff, T.V. Cunha, C.E. dos Santos, G. Lemos, Microstructural Characterization of an ERNiCrMo-3 and Grey Cast Iron Interface Obtained via TIG Welding, Metall. Mater. Trans. B. 53 (2022) 2534-2546.

[7] J.D. Hamilton, S. Sorondo, A. Greeley, X. Zhang, D. Cormier, B. Li, H. Qin, I.V. Rivero, Property-structure-process relationships in dissimilar material repair with directed energy deposition: Repairing gray cast iron using stainless steel 316L, J. Manuf. Process. 81 (2022) 27-34.

[8] M. Pouranvari, On the weldability of grey cast iron using nickel based filler metal, Mater. Des. 31 (2010) 3253-3258.

[9] L. Zhang, Filler metals, brazing processing and reliability for diamond tools brazing: A review, J. Manuf. Process. 66 (2021) 651-668.

[10] Y. Li, C. Chen, R. Yi, Y. Ouyang, Review: Special brazing and soldering, J. Manuf. Process. 60 (2020) 608-635.

[11] P.T. Vianco, A Review of interface microstructures in electronic packaging applications: Brazing and welding technologies, J.O.M. 74 (2022) 3557-3577.

[12] J. Chen, X. Wang, X. Li, N. Li, Q. Yang, Effects of brazing temperature and holding time on wettability of brazing diamond and brazing interface analysis, Weld. World. 64 (2020) 1763-1770.

[13] P.M. Roberts, An introduction to vacuum furnace brazing technology - Part 2: Further technical considerations and brazing hardware, Weld. Cut. 18 (2019) 30-34.

[14] K. Waetzig, J. Schilm, S. Mosch, W. Tillmann, A. Eilers, L. Wojarski, Influence of the brazing paste composition on the wetting Behavior of reactive air brazed metal - ceramic joints, Adv. Eng. Mater. 23 (2021) 2000711.

[15] M.M. Schwartz, Brazing, ASM International, 2003.

[16] A.F. Looty, F.A. Hashim, S.K. Hussein, Effect of sliver filler metal alloy on bonding structure for brazing Ni270 to Ductile cast iron, OP Conf. Ser.: Mater. Sci. Eng. 881 (2020) 012060.

[17] S. Katayama, Laser Welding, Joining, or brazing of Dissimilar Materials, in Topics in Mining, Metallurgy and Materials Engineering, 2020.

[18] ASTM E8M, Standard Test Methods for Tension Testing of Metallic Materials, American Society for Testing and Materials, 2016.

[19] ASTM E384, Standard test method for Knoop and Vickers hardness of materials, American Society for Testing and Materials, 2011.

[20] ASTM G5, Standard reference test method for making potentiostatic and potentiodynamic anodic polarization measurements. American Society for Testing and Materials, 2004.

[21] G. Krauss, Steel: Heat Treatment and Processing Principles, ASM International, 1990.